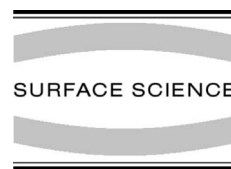




ELSEVIER

Surface Science 493 (2001) 453–459



www.elsevier.com/locate/susc

# Scanning tunneling microscopy and X-ray photoelectron spectroscopy of silver deposited octanethiol self-assembled monolayers

T. Ohgi \*, D. Fujita, W. Deng, Z.-C. Dong, H. Nejoh

*National Research Institute for Metals, 1-2-1, Sengen, Tsukuba 305, Japan*

Received 2 October 2000; accepted for publication 21 February 2001

## Abstract

Ag deposited self-assembled monolayers (SAMs) of octanethiol ( $\text{CH}_3(\text{CH}_2)_7\text{SH}$ ) have been studied using scanning tunneling microscopy and X-ray photoelectron spectroscopy (XPS). At the initial stage of Ag deposition, monatomic height islands,  $\sim 7 \times 10^{11} \text{ cm}^{-2}$  in density, grow at the SAMs/Au(111) interface and become larger as more Ag atoms are deposited up to a full monolayer coverage of Ag. The differences of the nucleation density and the growth property between Ag and Au islands can be attributed to the higher mobility of Ag atoms and the difference of the molecular packing on these islands. XPS analysis of this structure (SAMs/Ag monolayer/Au) shows that the Ag  $3d_{5/2}$  binding energy is shifted  $-0.3 \text{ eV}$  with respect to bulk Ag, the C 1s binding energy is  $\sim 0.3 \text{ eV}$  higher than that before Ag deposition, and the S  $2p_{3/2}$  binding energy exhibits little shift before and after deposition. The origin of the shift can be explained by the change of the dipole at the interface and the electrical isolation of alkyl chains from the surroundings. © 2001 Elsevier Science B.V. All rights reserved.

**Keywords:** Scanning tunneling microscopy; X-ray photoelectron spectroscopy; Epitaxy; Self-assembly; Surface diffusion; Silver

## 1. Introduction

The self-assembled monolayers (SAMs) of thiol molecules on Au(111) have attracted much attention because of the simplicity of preparation and their applicability. Especially, the applications as tunnel barriers and insulating layers are expected in the field of the nanoscale electronics, because the film thickness can be precisely controlled on the atomic scale by changing the length

of molecules. The interface structure between SAMs and substrates and the interaction between SAMs and deposited metal overlayers are therefore of great importance in this field and a lot of researches about the structures [1–4] and the electrical transport properties of metal/SAMs/metal heterostructures have been reported [5–8]. Moreover this could be a good model for the fundamental studies of organic molecules and metal atoms in their interacting systems since the structure is very simple and the obtained results can be easily interpreted due to the well defined and very simple structure on the atomic scale.

In the previous paper [9], we studied gold deposited SAMs of octanethiol ( $\text{CH}_3(\text{CH}_2)_7\text{SH}$ ) on

\* Corresponding author. Tel.: +81-298-59-2789; fax: +81-298-59-2701.

E-mail address: ohgi.taizo@nims.go.jp (T. Ohgi).

Au(111) using scanning tunneling microscopy (STM). Deposited Au atoms cannot stay on the surface of layers, but penetrate through them and form monatomic height islands at the interface between SAMs and Au(111) substrate after sub-monolayer deposition. In this system, the molecules act as surfactants and hinder the diffusion of metal atoms, resulting in the high nucleation density ( $\sim 2 \times 10^{12} \text{ cm}^{-2}$ ) and different growth characteristics from the normal metal-on-metal epitaxial growth.

In this paper, we report the results of Ag deposition on the SAMs of octanethiol. The surfaces were studied by STM and X-ray photoelectron spectroscopy (XPS). Ag coverage dependence of the morphology with photoelectron spectroscopy analysis is shown and the difference of the growth property of Ag islands from that of Au is discussed. After Ag deposition monatomic height islands grow at the SAMs/Au(111) interface and SAMs/Ag monolayer/Au(111) structure can be obtained. This could be useful to monitor local electronic states of the topmost atoms (Ag) with which sulfur atoms of alkanethiol are bound, and also to study the enhancement of the thermal stability of SAMs which has been reported recently [10,11].

## 2. Experiment

Au(111) with a thickness of  $\sim 100 \text{ nm}$  and a terrace size of around  $100 \text{ nm}$  on mica were used for substrates. The preparation method of substrates and SAMs is the same as the previous report [9]. As reported in many other papers [12–14], Au(111) terraces covered with SAMs have many pits of a monatomic depth and SAMs have many domains. The density and the occupation percentage of pits in our samples are  $\sim 1 \times 10^{12} \text{ cm}^{-2}$  and  $\sim 7\%$ , respectively. The density of SAMs domains is almost the same as that of pits. The surface is mostly covered with closely packed molecules and there are few defects in the SAMs except at domain boundaries. Ag was deposited on the SAMs by a resistive heat evaporator at a rate of  $0.01 \text{ ML (monolayer)/s}$ . The distance between sample and Ag source is set to  $\sim 40 \text{ cm}$  for the

suppression of heat radiation effect. All images were taken by air-STM (JEOL Ltd., JSTM-4200S) in the constant current mode with  $+1.0 \text{ V}$  bias voltage (sample biased) and  $40 \text{ pA}$  tunneling current, typically. STM tips were made by mechanically cutting a PtIr (10% Ir) wire. The surfaces were also analyzed by XPS (PHI 5400) using  $\text{MgK}\alpha$  X-ray ( $1253.6 \text{ V}$ ) operating at  $200 \text{ W}$ . The spectra were acquired with a pass energy of  $35.75 \text{ eV}$ . The overall energy resolution (FWHM) is  $\sim 0.9 \text{ eV}$  in this measurement conditions. The binding energy scales were referenced to the  $\text{Au } 4f_{7/2}$  ( $84.0 \text{ eV}$ ). The positions of the binding energy and the intensities were determined by least-squares curve fitting with Gaussian–Lorentzian product function [15].

## 3. Results and discussion

### 3.1. Scanning tunneling microscopy

Fig. 1 shows images after the vapor deposition of Ag onto SAMs/Au(111) surfaces. At the initial stage of Ag deposition Ag atoms grow into monatomic height islands,  $\sim 7 \times 10^{11} \text{ cm}^{-2}$  in density. As more Ag atoms are deposited the islands grow laterally (b), coalesce with the neighbor islands (c and d), form network structure (e) and fully cover the surface with Ag monolayer (f). At the coverage of  $0.5 \text{ ML}$  some islands grow from Au(111) step edges and surround most of the terraces (d). From these STM results together with XPS analysis shown later, it can be concluded that the deposited silver atoms penetrate through the SAMs and form islands at the SAMs/Au(111) interface. Although this phenomenon is similar to that of Au deposited SAMs [9], there exist some differences as summarized in Table 1.

When submonolayer Ag atoms are deposited on a clean Au(111) surface, islands on terraces as seen in the figures are not observed but most of Ag atoms stick to Au step edges [16], indicating that thiol molecules hinder the motion of Ag as well as that of Au. The density of the grown Ag islands is, however, about one-third of that of Au islands after Au deposition ( $\sim 2 \times 10^{12} \text{ cm}^{-2}$ ) [9]. Because we deposited Au and Ag on SAMs/Au with the

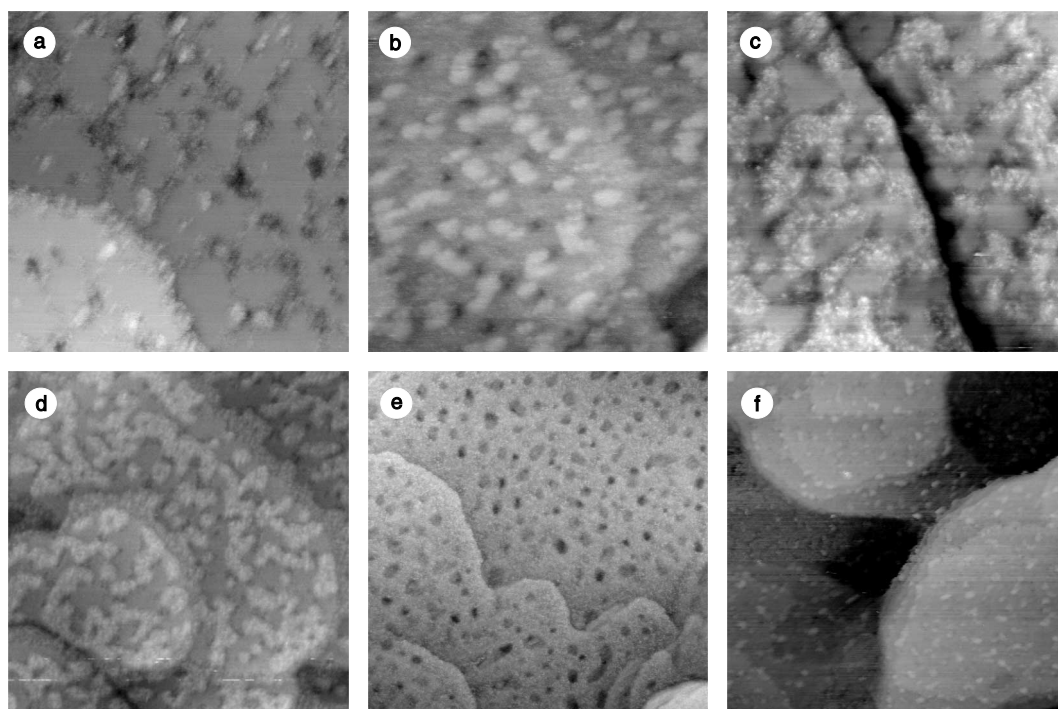


Fig. 1. STM images of octanethiol SAMs after (a) 0.1 ML, (b) 0.2 ML, (c) 0.4 ML, (d) 0.5 ML, (e) 0.7 ML and (f) 1.1 ML Ag deposition. The area size is  $110 \times 110 \text{ nm}^2$  in (a–c) and  $215 \times 215 \text{ nm}^2$  in (d–f).

Table 1

The density and the growth property of Au and Ag islands at SAMs/Au(1 1 1) interface

$\times 10^{12} \text{ cm}^{-2}$	Au <sup>a</sup>	Ag
Density of pits at 0 ML	~1	~1
Density of grown islands at initial deposition	~2	~0.7
Density of pits after coalescence at 0.7 ML	>2.5	<0.6
Growth of second layer starts	Before full coverage of first layer	After full coverage of first layer

<sup>a</sup> From Ref. [9].

same deposition rate (0.01 ML/s) and temperature, the difference in the nucleation density can be attributed to higher mobility of Ag atoms than Au in this system. At present, however, we are not yet able to describe the mechanism of the diffusion and the nucleation of deposited atoms in detail: whether they diffuse on the surface of SAMs or at

SAMs/Au(1 1 1) interface. In the former case, the interaction with topmost  $-\text{CH}_3$  and the packing of SAMs are important, while in the latter case the interaction with the substrate and sulfur atoms of  $-\text{S}-\text{Au}$ , and the intermolecular interaction affect the mobility.

After the formation of network structure (Fig. 1(e)), uncovered areas are left as pits with a density close to that of the initially grown islands. About 30% of these pits have a double atomic depth, indicating that the original pits are not filled out completely. However, this growth property is not applicable to the second layer, which starts to grow after the first layer covers the whole surface (i.e., after filling out single and double atomic depth pits) (Fig. 1(f)). On the other hand, in the case of Au deposited surfaces, some pits have double atomic depth after coalescence of the first layer in the same way, but the second layer starts to grow *before* the first layer fully covers the surface. One possible explanation for this difference is

that the mobility of Ag atoms at SAMs/Ag interface is higher than that at the SAMs/Au interface. This is based on the assumption that the islands at the interface are formed at the early stage of Ag deposition and the subsequently deposited atoms diffuse at both SAMs/Ag and SAMs/Au interfaces. The difference of the bonding energies between  $-S-Au$  and  $-S-Ag$  or the different packing of molecules as shown later must play an important role. The density of the second layer islands does not exhibit apparent differences from that of the first layer islands, which is not expected if we assume different mobility at SAMs/Au and SAMs/Ag interfaces. However, after Ag deposition, the density of original pits is reduced to  $\sim 20\%$ , suggesting that the original pits also trap diffusing Ag atoms and the real nucleation density of the first layer is higher than that of the second layer. Another possible explanation for the full coverage of the Ag first layer is related to the surface tension or the surface free energy of the SAMs/Ag system. This is probably a much slower process than the nucleation of the islands. As reported in the previous paper [9], densely packed SAMs stabilize the structure underneath, while the islands is not stable under disordered SAMs. The ordered structure of SAMs on the grown Ag islands are destroyed as shown later, which might cause Ag atoms to diffuse and cover Au completely.

Although on Au deposited surfaces ordered structures of molecules are observable on both original terraces and grown islands, on Ag deposited surfaces ordered structures are seen only on the area where Ag islands are not grown. As shown in Fig. 2, the distribution of height from each pixel indicates that the roughness of the surface is enhanced. As shown in Fig. 1(d), the boundary between the original terraces and the surrounding Ag layer grown from step edges is clearly seen. In the case of Au deposited surfaces [9], no such boundary was observed. The different growth characteristic of Au and Ag islands at the interfaces suggests that there exist differences in the bonding property between a sulfur atom and metal substrate (Ag or Au) even though their lattice constants are very similar. Moreover, recent diffraction and STM studies have shown that the nearest neighbor spacing of SAMs on Ag(111) is

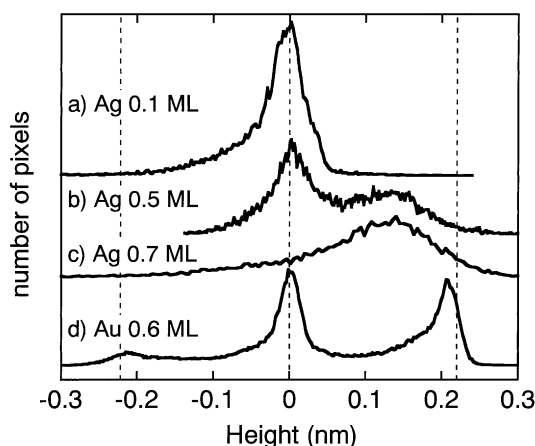


Fig. 2. Height distribution of SAMs/Au(111) surface after (a) 0.1 ML (b) 0.5 ML (c) 0.7 ML Ag deposition and (d) 0.6 ML Au deposition. Only one terrace is selected from Fig. 1 to remove the overlap of the height distribution between terraces. The distribution (d) is from Fig. 2(c) in Ref. [9].

shorter than that on Au(111) [17] ( $\sim 4.7$  Å for SAMs/Ag(111) and  $\sim 5$  Å for SAMs/Au). Because the number of molecules should be conserved even after Ag deposition, the density of thiol molecules of our SAMs/Ag monolayer/Au(111) structure is at least 10% less than that of SAMs/Ag(111), which might cause inequilibrium condition of molecules on Ag islands and possibly is the origin of the roughness. This situation is totally different from recently reported results where SAMs are formed after covering Au(111) with Ag monolayer [18].

### 3.2. X-ray photoelectron spectroscopy

The analysis by XPS was performed to examine the core level shift and the change of spectra intensities of Au 4f, Ag 3d, C 1s and S 2p. No oxygen (O 1s) was detected for original and Ag deposited samples even after the exposure to air for a few hours at least. As Ag coverage increases, the intensity of Ag 3d ( $I_{Ag}$ ) increases and that of Au 4f ( $I_{Au}$ ) decreases monotonically, while the intensities of C 1s ( $I_C$ ) and S 2p ( $I_S$ ) remain almost constant. The intensity ratio,  $I_C/I_S$ , are not changed even after Ag deposition and STM observations, indicating that the influence of the

contamination on C 1s spectra is negligible.  $I_{\text{Ag}}/I_{\text{C}}$  exhibits the strong dependence on the photoelectron take-off angle ( $\theta$ ).  $(I_{\text{Ag}}/I_{\text{C}})_{\theta=90^\circ}/(I_{\text{Ag}}/I_{\text{C}})_{\theta=24^\circ}$  is  $\sim 1.5$  while  $(I_{\text{S}}/I_{\text{C}})_{\theta=90^\circ}/(I_{\text{S}}/I_{\text{C}})_{\theta=24^\circ}$  is  $\sim 1.4$ . This means that Ag layers really grow at the SAMs/Au interface. From the Ag coverage dependence of  $I_{\text{Au}}$ , the attenuation length ( $\lambda$ ) of Au 4f photoelectrons (kinetic energy  $\sim 1170$  eV) through the Ag layer is estimated to be  $\sim 7.6$  ML, in good agreement with previous report [19].

The Ag coverage dependence of the core level shift of Ag  $3d_{5/2}$ , C 1s and S  $2p_{3/2}$  is shown in Fig. 3. It is seen that the Ag  $3d_{5/2}$  binding energy shifts  $-0.3$  eV with respect to that of bulk Ag. The C 1s binding energy shifts positively with increasing Ag coverage ( $\sim 0.3$  eV upon 1 ML deposition) and the S  $2p_{3/2}$  binding energy exhibits little shift from that before deposition. Former two results are similar to the reported ones [1].

Because the electronegativity of gold and silver and the work functions of those (111) planes are different, it is anticipated that the silver deposition causes the change of electron distribution at the interface. However, this effect seems to be not significant for sulfur atoms of SAMs, large shift is not observed. This result is reasonable because the binding energy of S 2p of SAMs on Au(111) and that on bulk Ag(111) are almost same,  $\sim 161.9$  eV. On the other hand, the binding energy of Ag atoms grown at the interface is greatly shifted in comparison with that of the bulk. The interaction with the Au(111) substrate and the formation of  $-S-Ag$  bonding might be the possible origin of this shift. To discuss the effect of sulfur atoms on this shift in detail, the data without molecules is necessary, which has not been systematically studied yet. However, the binding energy in our experiment is in good agreement with reported one where SAMs were formed on the underpotentially deposited Ag monolayer [11]. Hence from this together with the evidence described above it can be concluded that SAMs are formed on Ag(1 ML)/Au(111).

Since S  $2p_{3/2}$  shows little shift (that is, little change of the electron density around sulfur atoms) and alkyl chains are connected to substrate via sulfur atoms, it is hard to ascribe the shift of C 1s to the charge transfer. Considering STM ima-

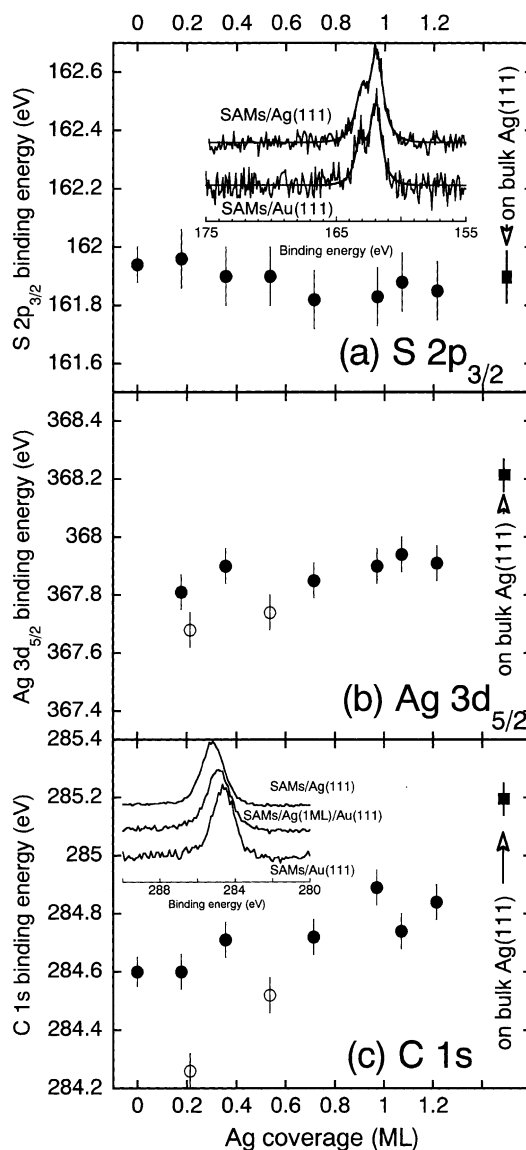


Fig. 3. The Ag coverage dependence of the core level shift of S  $2p_{3/2}$  (a), Ag  $3d_{5/2}$  (b) and C 1s (c) (●). Solid rectangles denote the binding energies obtained from SAMs/Ag(111). Open circles are from slightly oxidized samples. (0.2 and 0.5 ML Ag deposited samples were exposed to air for seven and four days, respectively.) Inset in (a): XPS spectra of S 2p from SAMs on Ag(111) and Au(111) substrate. Inset in (c): XPS spectra of C 1s from SAMs/Ag(111), SAMs/Ag(1 ML)/Au(111) and SAMs/Au(111).

ges, one possible explanation for this shift is the morphological change of SAMs on Ag islands

which might be related to the intermolecular interaction or the packing of alkyl chains. However the positive shift is in contrast with the results reporting that the C 1s binding energy of molecules becomes lower when the alkyl chains are disordered (or less dense) [20–22]. In addition, our STM images clearly exhibit the domain separation between SAMs on Au and those on Ag. The existence of the two types of alkyl chains on the same substrate would cause the coupling of two spectra. However, this broadening of the C 1s spectrum (FWHM  $\sim 1.4$  eV) is not observed in our experiment which shows little Ag coverage dependence. The C 1s binding energy of SAMs on bulk Ag(111) is  $\sim 285.2$  eV (FWHM  $\sim 1.4$  eV), 0.6 eV higher than that on Au(111), which seems to follow the general interpretation: the higher lateral chain density, the higher C 1s binding energy. However, this simple interpretation is not based on the theoretical reasoning and seems to still have a problem.

Another possible explanation for C 1s shifts is the reformation of dipole layers at the SAMs/Au interface by Ag deposition as suggested by Tarlov [1]. Semiempirical molecular orbital calculation shows that the highest occupied molecular orbital (HOMO) of alkanethiol exists around sulfur atom and that the electron injection and withdrawal through sulfur atoms, such as oxidization of S atom, little affects the density of electron at the alkyl chains. Due to the chemical bonding between the metal substrate and sulfur atoms, the hybridization between HOMO around S atoms and surface electrons occurs and would lead to the interface dipole, while in alkyl chain the reformation of electron distribution is negligible.

In order to check the interface dipole effect further, we also examine the samples with the interface slightly oxidized. Ag deposited samples are spontaneously oxidized by the exposure to air for a few days and causes the decrease of Ag 3d and C 1s binding energy as shown in Fig. 3. (Note that the oxidization of Ag leads to a negative shift of Ag 3d<sub>5/2</sub> binding energy [23].) The origin of the shift can be ascribed to the increase of the work function due to the oxidization of Ag at the interface, which is also seen in the porphyrin/Ag system [24]. This is not the effect of sulfur oxidization,

because the C 1s shift like this is not seen in the SAMs/Au(111) system where only sulfur atoms can be oxidized. The systematical studies with the direct observation of the work function change will give us more insights about the dipole layer formation at the chemisorbed interface.

#### 4. Conclusion

We have studied Ag deposited SAMs of octanethiol molecules ( $\text{CH}_3(\text{CH}_2)_7\text{SH}$ ) by STM and XPS. Similar to Au deposited SAMs, it was found that deposited Ag atoms penetrate through SAMs and form monatomic height islands underneath. Lower nucleation density of Ag islands suggests that Ag atoms in the SAMs/Au(111) system have a higher mobility than Au atoms. In contrast to the Au deposited SAMs, the ordered structure of SAMs on grown Ag islands is destroyed while the ordered structure is conserved at the area where Ag islands are not grown. Instead of the general expectation, the anomalous positive shifts of C 1s binding energy were observed. The constant FWHM and the domain separation in STM images imply that the possible dipole layer is formed at the narrow interface region which does not include alkyl chains.

#### Acknowledgement

The authors are grateful to Dr. M. Yoshitake for her valuable help in XPS measurements.

#### References

- [1] M.J. Tarlov, *Langmuir* 8 (1992) 80.
- [2] E.L. Smith, C.A. Alves, J.W. Andereg, M.D. Porter, L.M. Siperko, *Langmuir* 8 (1992) 2707.
- [3] G.C. Herdt, A.W. Czanderna, *J. Vac. Sci. Technol. A* 17 (1999) 3415.
- [4] D.R. Jung, A.W. Czanderna, G.C. Herdt, *J. Vac. Sci. Technol. A* 14 (1996) 1779.
- [5] D. Anselmetti, T. Richmond, A. Baratoff, G. Borer, M. Dreier, M. Bernasconi, H.-J. Güntherodt, *Europhys. Lett.* 25 (1994) 297.
- [6] M. Dorogi, J. Gomez, R. Osifchin, R.P. Andres, R. Reifemberger, *Phys. Rev. B* 52 (1995) 9071.

- [7] C. Baulas, J.V. Davidovits, F. Rondelez, D. Vuillaume, *Phys. Rev. Lett.* 17 (1996) 4797.
- [8] C. Zhou, M.R. Deshpande, M.A. Reed, J. Jones II, J.M. Tour, *Appl. Phys. Lett.* 71 (1997) 611.
- [9] T. Ohgi, H.-Y. Sheng, Z.-C. Dong, H. Nejoh, *Surf. Sci.* 442 (1999) 277.
- [10] G.K. Jennings, P.E. Laibinis, *Langmuir* 12 (1996) 6173.
- [11] G.K. Jennings, P.E. Laibinis, *J. Am. Chem. Soc.* 119 (1997) 5208.
- [12] E. Delamarche, B. Michel, Ch. Gerber, D. Anselmetti, H.-J. Güntherodt, H. Wolf, H. Ringsdorf, *Langmuir* 10 (1994) 2869.
- [13] G.E. Poirier, M.J. Tarlov, *Langmuir* 10 (1994) 2853.
- [14] C. Schönenberger, J.A.M. Sontag-Huethorst, J. Jorritsma, L.G.J. Fokkink, *Langmuir* 10 (1994) 611.
- [15] P.M.A. Sherwood, in: D. Briggs, M.P. Seah (Eds.), *Practical Surface Analysis*, second ed., vol. 1, Wiley, Chichester, 1990.
- [16] M.M. Dovek, C.A. Lang, J. Nogami, C.F. Quate, *Phys. Rev. B* 40 (1989) 11973.
- [17] A. Dhirani, M.A. Hines, A.J. Fisher, O. Ismail, P. Guyot-Sionnest, *Langmuir* 11 (1995) 2609.
- [18] M.-H. Hsieh, C.-H. Chen, *Langmuir* 16 (2000) 1729.
- [19] M.P. Seah, W. Dench, *Surf. Interf. Anal.* 1 (1979) 2.
- [20] J. Thome, M. Himmelhause, M. Zharnikov, M. Grunze, *Langmuir* 14 (1998) 7435.
- [21] T. Ishida, M. Hara, I. Kojima, S. Tsuneda, N. Nishida, H. Sasabe, W. Knoll, *Langmuir* 14 (1998) 2092.
- [22] H.-J. Himmel, Ch. Wöll, R. Gerlach, G. Polanski, H.-G. Rubahn, *Langmuir* 13 (1997) 602.
- [23] J.F. Moulder, W.F. Stickle, P.E. Sobol, K.D. Bomben, *Handbook of X-ray Photoelectron Spectroscopy*, Physical Electronics Ins., Minnesota, 1995.
- [24] S. Narioka, H. Ishii, D. Yoshimura, M. Sei, Y. Ouchi, K. Seki, S. Hasegawa, T. Miyazaki, Y. Harima, K. Yamashita, *Appl. Phys. Lett.* 67 (1995) 1899.